Polyelectrolyte Adsorption onto Insoluble Monolayers at the Air/Water Interface

Heiko Ahrens,[†] Hubert Baltes,[†,‡] Johannes Schmitt,[†] Helmuth Möhwald,[‡] and Christiane A. Helm*[,†,§]

Institut für Physikalische Chemie, Johannes Gutenberg-Universität, Jakob-Welder Weg 11, D-55099 Mainz, Germany; MPI für Kolloid- und Grenzflächenforschung, D-14424 Golm, Germany; and Angewandte Physik, Universität Greifswald, Friedrich-Ludwig-Jahn-Str. 16, D-17487 Greifswald, Germany

Received August 31, 2000; Revised Manuscript Received March 5, 2001

ABSTRACT: Poly(styrenesulfonate) (PSS) was adsorbed reversibly from aqueous CsCl or NaCl solutions onto oppositely charged DODAB (diocatadecyldimethylammonium bromide) monolayers at the water surface. By adjusting the DODAB lateral density, the surface charge of the liquid interface is varied. The electron density profile of the surface layer was measured with X-ray reflectivity, using counterion contrast. A flat PSS layer is always found, with a thickness corresponding to one to two chain diameters. At low surface charge, the PSS coverage is constant and large, presumably due to hydrophobic attraction. A surface charge overcompensation of up to 6:1 is observed. The PSS coverage increases both with surface charge and with ionic strength. Intriguingly, at high salt (1 M) and low surface charge, beneath the flat concentrated PSS layer a diffuse extended adsorption layer is found. Its thickness decreases on increase of the surface charge and disappears at ca. 80 Å^2 DODAB molecular area, causing a minimum in PSS coverage. The diffuse extended layer is not found for a short PSS with 52 Å contour length.

Introduction

Polymers near interfaces have gained tremendous interest for technical reasons.[1,2] Specifically, charged polymers (polyelectrolytes) are used in many processes like flocculation, colloid stabilization, or fabrication of multilayer films and coating,[1,2] and although theories will have to wait with a detailed understanding, they will require dedicated experiments in a well-defined geometry[3] to clarify the energetic as well as molecular arrangement. Polyelectrolytes being a most important class of polymers are theoretically even more demanding as neutral polymers because of the existence of long- or short-range electrostatic forces, depending on the ionic strength.[4]

Force measurements between liquid surfaces indicate polyelectrolyte layering[5] while between solid surfaces irreversible adsorption is found.[6−10] Lateral structure of polyelectrolytes adsorbed to solid surfaces is even indicated by some experiments.[11] The liquid interface consists of a self-organzing monolayer of water-soluble amphiphiles. The lateral mobility of the amphipiles explains the short equilibration times (minutes to hours) of fluid interfaces; relaxation times on solid surfaces amount to a few days.[3] Yet, there are general trends observed in all surface forces experiments: low ionic strength yields flat polyelctrolyte adsorption,[10,11] while high ionic strength causes a more extended (coiled) adsorption.[8,9]

This work considers the interaction of two most frequently investigated systems: monolayers of the saturated double-chain amphiphiles DODAB[12,13] interacting with the strong polyelectrolyte PSS.[4] This enables us to compare the results with literature data on certain aspects, and it also enables future dedicated experiments, because many structural variants of these compounds are available. Special attention is paid in this work to resolve the polyelectrolyte distribution along the surface normal as a function of lipid charge density, polymer molecular mass, and ionic strength.

A most suitable model system to study interfaces are monolayers at the air/water interface made of insoluble amphiphiles[14] of defined charge density in contact with polyelectrolyte in the subphase. They enable continuous variation of the surface charge as well as direct measurement of the interface energetics.[15] The lateral lipid mobility enables establishment of equilibrium on much shorter time scales than after adsorption on solid support and through air the interface is easily accessible to light, X-ray, and neutron beams.

Even though conventional X-ray tubes already offer a much higher brilliance than international neutron sources, X-rays are little used in polymer science because of contrast problems. Solvent and polymer exhibit almost the same electron density. To circumvent this problem with polyelectrolytes, we suggested the method of counterion labeling.[16] It is based on the prediction of the DLVO theory that 95% of the surface charge neutralizing ions are within one ionic diameter of the surface[17] and the rest close by. Therefore, electron-rich counterions can be used as labels for the adsorbed polyelectrolyte. Obvously, to exclude ion specifity, different counterions have to be used.

Materials and Methods

DODAB (cf. Figure 1) served as a positively charged amphiphile. PSS with two different molecular weights was used as oppositely charged polyelectrolyte (PSS, Polymer

[†] Johannes Gutenberg-Universität.
[‡] MPI für Kolloid- und Grenzflächenforschung.
[§] Universität Greifswald.
* To whom correspondence should be addressed. E-mail helm@physik.uni-greifswald.de.

10.1021/ma001520h CCC: $20.00
Published on Web 05/25/2001

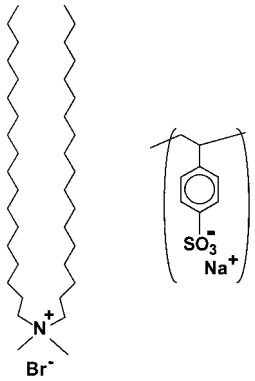

Figure 1. Structure formulas of DODAB and PSS.

Standard Service, Mainz, Germany), 77 400 and 4300 Da (377 and 21 monomer units, 943 and 52 Å contour length, respectively), with $M_w/M_n < 1.05$. Ultrapure water was from Millipore (Milli-Q), and the salts NaCl and CsCl (99%) were from Merck (Darmstadt, Germany). To prepare an insoluble monolayer, DODAB was dissolved in chloroform (1 mg/mL) and about 100 μL spread on the aqueous solution. The polyelectrolyte concentration was kept constant throughout our experiments, 10^{-3} mol (to be exact: 10^{-3} monomers/L).

The X-ray setup is home-built[18] with a Cu anode (wavelength $\lambda = 1.54$ Å). In X-ray experiments, the index of refraction n depends linearly on the electron density ρ and known constants (Thomson radius r_0), $n = 1 - r_0\rho\lambda^2/2\pi$, and deviates only by 10^{-5} from 1. Therefore, approximations are possible, and basically, the measured reflectivity R is the Fresnel reflectivity R_F of an infinitely sharp interface modulated by interference effects from the thin surface layer.[19] Above about two critical angles the reflectivity can be described by the kinematic approximation $R/R_F = |(1/\rho_{sub})\int \rho'(z) e^{iQ_z z}\, dz|^2$, where ρ_{sub} is the electron density of the bulk phase, $\rho'(z)$ the gradient of the electron density along the surface normal, and Q_z the wave vector transfer normal to the surface. For a 0.1 M CsCl subphase $\rho_{sub} = 0.3373$ e$^-$/Å, which is larger than that of clean water (0.333 e$^-$/Å) due to the electron-rich Cs^+ ions. The electron density profiles were calculated first by an indirect Fourier transform of the master formula.[20,21] Then, to quantify the molecular parameters, the exact matrix formalism is used.[22] The surface layer is parametrized as consisting of different slabs (each with an electron density and a thickness as well as a roughness parameter). In all cases, the simulated reflectivity is convoluted with the anugular divergence (0.012°). The electron density profiles obtained in this manner coincide within error with the profiles obtained by indirect Fourier transform, as found previously. To recognize and possibly eliminate correlated parameters, a sensitivity analysis of the interdependency of the parameters is also performed.[23]

Before X-ray reflectivity experiments were started, one isotherm was measured with a slow compression speed, 0.1 Å^2/(molecule s). Then the film was totally expanded. Reflectivity experiments were performed during the second compression, at preselected molecular areas. Before exposure to X-rays, the monolayer was allowed to relax for 30 min, and then the reflectivity measurement started.

Results

Amphiphilic Monolayer on Different Ionic Strengths Solutions. A pure DODAB monolayer was investigated first, with different NaCl concentrations in the water (0, 0.01, 0.1, 0.5, and 1 M). All the isotherms depicted in Figure 2 are similar and in good agreement with the literature:[12,24] The onset of an expanded phase is characterized by a pressure increase at 105−125 Å^2/molecule. A plateau region indicates a first-order phase transition which starts at ca. 80 and ends at 60

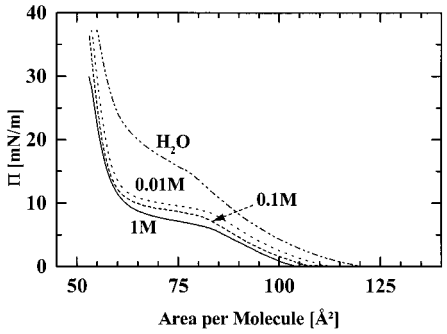

Figure 2. Isotherms of pure DODAB (20 °C) on NaCl solutions (from ref 57).

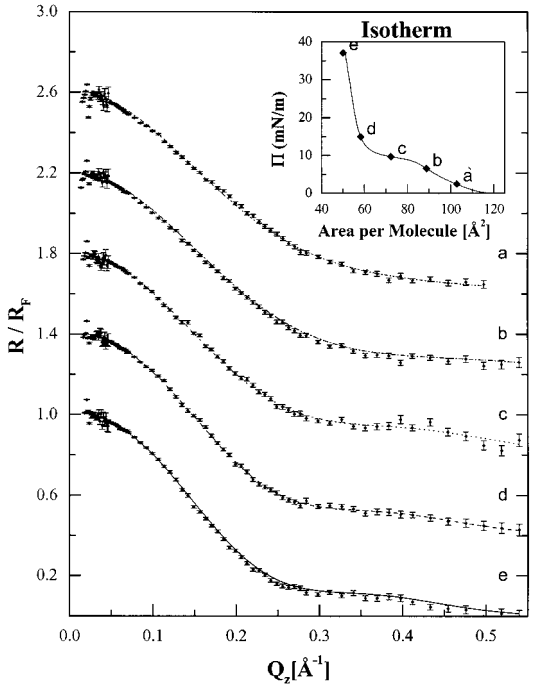

Figure 3. Normalized X-ray reflectivity curves convoluted with the instrumental resolution of a DODAB monolayer on 0.1 M NaCl solution at the molecular areas indicated in the isotherm shown in the inset. For clarity, the X-ray reflectivity curves are displaced by 0.4.

Å^2/molecule. The compressed phase at high pressures was found to consist of stretched alkyl chains tilted by ca. 45° relative to the surface normal,[13] leading to a minimum molecular area of 55 Å^2/molecule. Compression/expansion hysteresis of the isotherms is small, about 1 mN/m.

With increasing salt concentration the isotherms are shifted to lower lateral pressure. This effect is especially obvious if one compares the onset of the plateau region[25−27] at ca. 80 Å^2/molecule. The lateral pressure decrease can be explained with progressive screening of the monolayer surface charge[28] and is, according to the Gouy−Chapman theory, consistent with the assumption that most of the DODAB molecules are charged.

The X-ray reflectivity curves obtained on 0.01, 0.1, and 1 M salt solution are very similar, with few interference maxima. A representative data set is depicted in Figure 3. The one with the clearest contrast is obtained for the highly compressed monolayer (curve e). A shoulder at 0.1 Å^{-1} is followed by a weak minimum at 0.25 Å^{-1} and a maximum at 0.4 Å^{-1}. With increasing

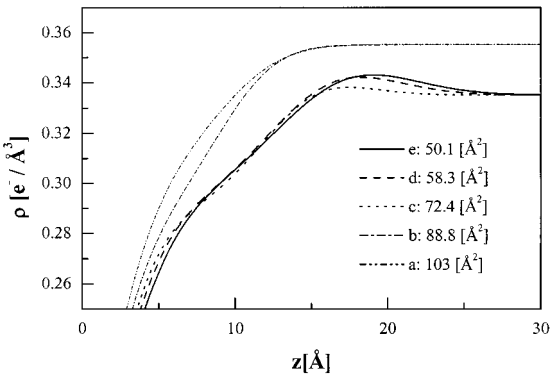

Figure 4. Electron density profiles for DODAB on 0.1 M NaCl solution at different molecular areas, corresponding to the reflectivity curves in Figure 3. $z = 0$ corresponds to the monolayer/air interface. For clarity, the profiles in the expanded phase (curves a, b) are vertically shifted by 0.02 $e^-/Å^3$.

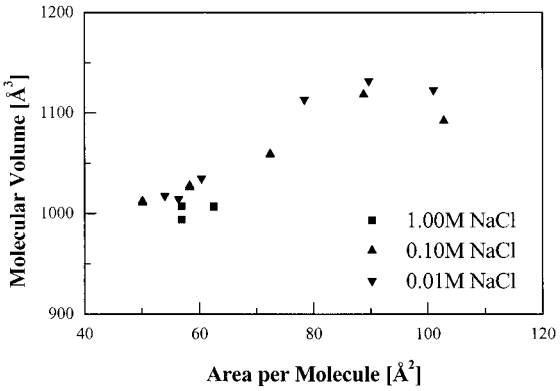

Figure 5. DODAB molecular volume as obtained by integrating along the electron density profiles according to eqs 1 and 2. Below a molecular area of ca. 60 $Å^2$ DODAB is in the condensed phase; above 80 $Å^2$ it is in the expanded phase. The decrease in molecular volume is obvious.

molecular area the minimum is shifted to larger Q_z, and the contrast weakens.

For other amphiphilic monolayers like phospholipids or fatty acids,[29−31] a two-slab model was often sufficient, with a high electron density slab for the hydrophilic headgroup and a second slab for the aliphatic tail groups. Depending on the phase of the alkyl chains, the electron density of the second slab is below or almost equal to the one of water.[32]

The weakly structured X-ray reflectivity curves (cf. Figure 3) yield rather unstructured electron density profiles (cf. Figure 4). It is impossible to distinguish an effect of the different salt solutions. Always, one common roughness for all interfaces is sufficient to yield good fits. In the expanded phase, one slab for the alkyl chains described the reflectivity curves satisfactorily; the headgroup could be detected only at the highest salt (1 M). It is easier to discern the headgroups in the compressed phase. However, the thickness and electron density of the headgroup cannot be determined independently. When the headgroup thickness is smaller than about twice the roughness, the maximum electron density found in the slab model depends strongly on the headgroup thickness. While the profile remains nearly unchanged, a thickness decrease of the headgroup layer is compensated in the simulations by an unphysically high electron density. It was impossible to overcome this ambiguity by assigning a fixed number of electrons to the tail slab (i.e., 274 e^- for two C_{17} tails), because the tail slab consists of fewer electrons.

To obtain some quantitative measure to describe the monolayer, the first derivative of the electron density profile is calculated. The separation between subsequent extrema is taken to be a slab length. It is interesting to note that all lengths are beneath 12 Å, even those for the most compressed ordered alkyl tails. Even with the large tilt angle of 45° (as found for DODAB alkyl chains in the crystal[13]), a slab thickness of 15 Å is expected. In contrast, the headgroup (10 Å) is longer than the molecular structure suggests. Therefore, a staggered headgroup conformation with interleaved counterions is suggested in the ordered phase, possibly with some kinks in the alkyl chains adjacent to the headgroups.

Yet, quantities that depend less on model assumptions are the molecular volume and the amount of electrons, because both can be determined directly by integrating along the z-axis from the air down into the water. It is important that the integration limits are far away from the molecule. The extremely well-defined tail/water interface is taken to be the point of origin, and l is the lower integration limit. Then, the volume lA is filled by the DODAB molecule, the Cl^- counterion, and an unknown amount of water.

$$lA = V_{\mathrm{DODAB}} + V_{\mathrm{Cl}} + n_{\mathrm{H_2O}} V_{\mathrm{H_2O}} \qquad (1)$$

The same molecules contribute the number of electrons

$$A\int_{-\infty}^{l} \rho(z)\, \mathrm{d}z = E_{\mathrm{DODAB}} + E_{\mathrm{Cl}} + n_{\mathrm{H_2O}} E_{\mathrm{H_2O}} \qquad (2)$$

In these equations, V_{DODAB} and $n_{\mathrm{H_2O}}$ are unknowns, with $V_{\mathrm{Cl}} = 33$ $Å^3$ and $V_{\mathrm{H_2O}} = 30$ $Å^3$. The number of water molecules $n_{\mathrm{H_2O}}$ is obviously a function of l. However, V_{DODAB} can be determined (cf. Figure 5). In the compressed phase a molecular volume V_{DODAB} of 1020 $Å^2$ is obtained, which corresponds to two ordered C_{20} alkyl chains and is very reasonable. In the expanded phase, the volume is increased by 10%, as expected for disordered alkyl chains. Apparently, the headgroup volume increases by a similar amount due to increased hydration. A similar 10% change of the molecular volume in DODAB monolayers was also observed ellipsometrically.[24]

Amphiphilic Monolayer on Polyelectrolyte Solutions. As the isotherms in Figure 6a show, a DODAB monolayer on a PSS subphase shows the same overall phase behavior with an expanded phase, a plateau region, and a condensed phase. It is very important to note that the isotherms we measure are equilibrium isotherms. The same isotherms are obtained if the DODAB monolayer was prepared on a PSS solution or if the isotherms are measured on a salt solution and the PSS was later added with a syringe.

With increasing salt concentration the first increase of the lateral pressure occurs at larger molecular areas (for 0.01, 0.1, and 1 M CsCl at 150, 200, and 300 $Å^2$, respectively), and the onset of the plateau region is increased by up to 10 mN/m. Thus, salt addition has the opposite effect as found without the plyelectrolyte, where increasing salt concentration caused the monolayer to condense (cf. Figure 2). Generally, due to PSS addition the hysteresis is increased by up to 3 mN/m (cf. Figure 6b). Very unexpectedly, if the shorter

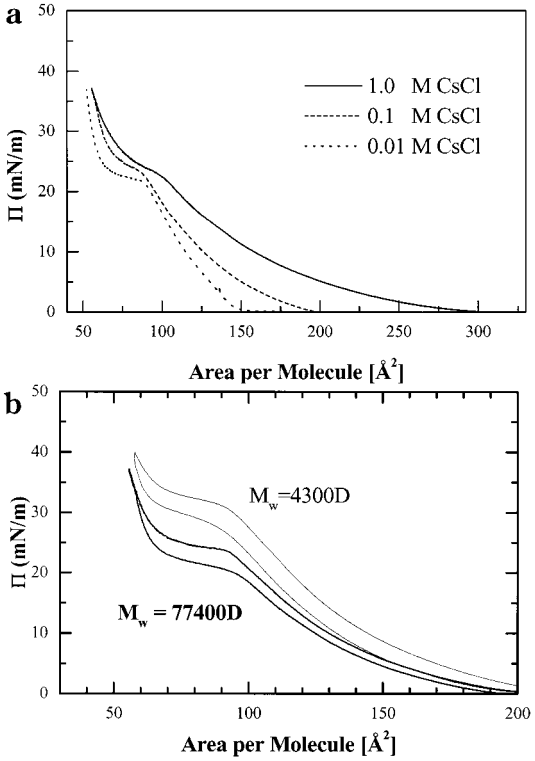

Figure 6. (a) DODAB compression isotherms on 10^{-3} mol/L PSS (M_w = 77 400) and CsCl concentrations as indicated. (b) Compression (top curve) and expansion (lower curve) cycles at 0.1 M CsCl and different molecular weight PSS. Bold lines and symbols are used to indicate the heavier polymer.

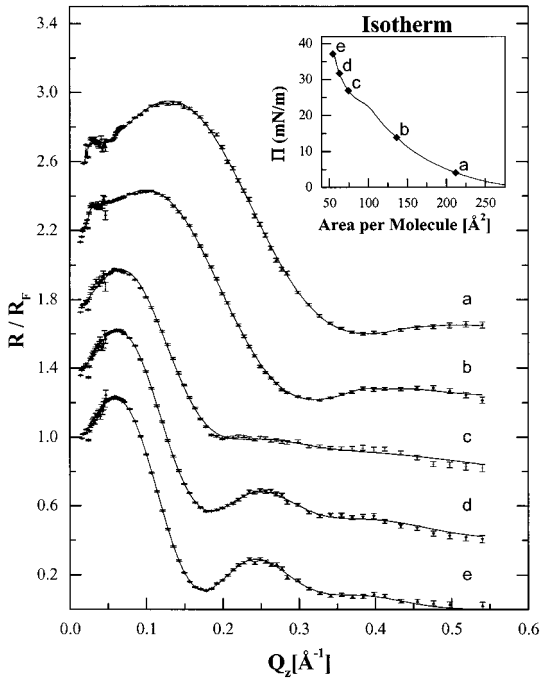

Figure 7. Normalized X-ray reflectivity curves convoluted with the instrumental resolution of a DODAB monolayer on 1 M CsCl and 0.001 mol/L PSS (M_w = 77 400) solution at the molecular areas as indicated in the isotherm shown in the inset. For clarity, the X-ray reflectivity curves are displaced by 0.4.

polymer is used, the lateral pressure is increased by another 8 mN/m while the molecular areas remain the same.

The X-ray reflectivity curves at large Q_z are very similar for all ionic strengths. A representative example is shown in Figure 7, an experiment on a 1 M CsCl subphase with 0.001 M PSS (M_w = 77 400 Da). In general, measurements on a CsCl subphase exhibit higher maxima compared to those on a NaCl subphase, indicating high surface ion concentrations. Compared to the experiments without PSS (cf. Figure 3), the reflectivity curves are much more structured; thus much more information can be obtained.

At very low Q_z (<0.04 Å^{-1}) and large molecular areas (curves a and b before the plateau region), a sudden jump in the reflectivity at the critical angle followed by a shallow minimum is observed. No further narrow oscillations are found. This indicates a thick polyelectrolyte layer with a very diffuse polymer/water interface. This thick polymer layer is only observed at 1 M salt concentration and for the long PSS (contour length 943 Å), not for the short PSS (contour length 52 Å). Generally, in the expanded phase a maximum at $Q_z \approx 0.1$ Å^{-1} occurs, which is typical for an electron-rich phase at the water adjacent side of the monolayer.[30,32] The following minimum measures the thickness of the low electron density alkyl chains.

On compression up to the plateau region, the extrema shift to lower Q_z values, indicating monolayer thickening. Also, the maxima shrink, indicating loss of electron density. This is very unusual. With all other monolayers investigated so far by other groups and us[18,29,31,32] contrast improvement on compression caused by headgroup dehydration was found. However, the main source of contrast in the experiments shown in Figure 7 is electron-rich Cs^+ ions. On compression they are apparently removed from the monolayer.

In the compressed phase, the interference at very low Q_z disappeared. The first maximum at $Q_z \approx 0.08$ Å^{-1} is very pronounced. At the beginning of the compressed region (curve c), the first minimum and the second maximum exhibit almost the same intensity, which causes a broad and slow decrease of the signal. On further compression, a second maximum ($Q_z \approx 0.25$ Å^{-1}) and even a third maximum ($Q_z \approx 0.4$ Å^{-1}) appear, which get more pronounced on decreasing the molecular area. Yet, the envelop of the three maxima is no simple Gauss function as one would expect from one roughness as derived in the slab model.[34]

Since the reflectivity curves in the expanded phase show little structure, only few parameters are necessary to describe an electron density profile. Concerning the lipid monolayer, one slab for the alkyl chains and one for the headgroup (PSS1 in the following text) would yield five free parameters (two thicknesses, two electron densities, and one roughness), which is more than can be deduced unambiguously. To have only four free parameters, as an additional constraint the amount of electrons in the tail slab was set to 274, corresponding to two C_{17} tails. Thus, the tail electron density is no longer a free parameter but can be calculated from the free parameter "tail thickness" and the molecular area from the isotherm. The very thick and rough polymer layer causing the interference directly at the critical angle is described by half a Gauss function (two additional parameters, one for the length and one for the electron density).

The more complex reflectivity profiles in the compressed phase (without the extended diffuse layer) necessitate another slab on the water side (called PSS2).

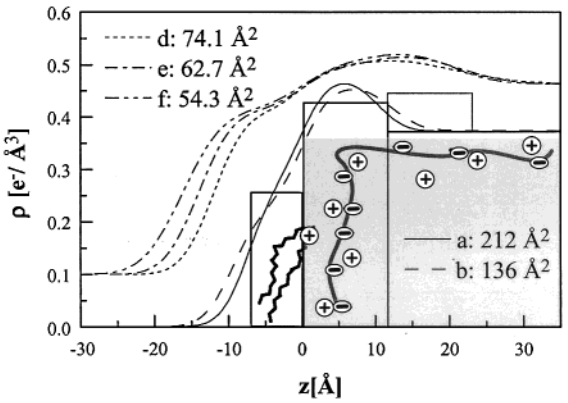

Figure 8. Electron density profiles of DODAB on 1 M CsCl and PSS solution at different molecular areas, corresponding to the reflectivity curves in Figure 7. $z = 0$ corresponds to the alkyl tails/headgroup interface. For clarity, the profiles in the condensed phase (curves d−f) are vertically shifted by 0.1 $e^-/Å^3$. Also shown is a schematic of the molecular arrangement within the slab model (tail slab, PSS1 and PSS2 slabs). The thick and diffuse polymer layer (≈70 Å) is indicated by the slightly increased electron density beneath the monolayer compared to the salt solution (shaded); it exceeds the scale of the figure.

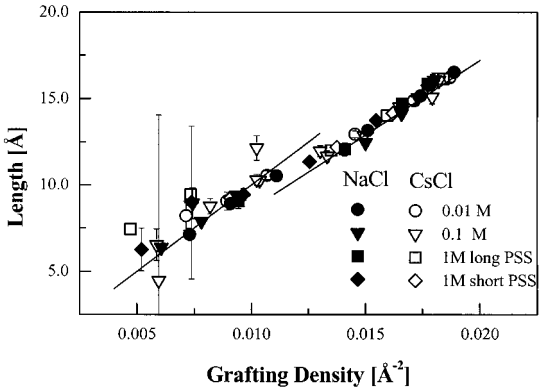

Figure 9. Length of the lipid chains as a function of the DODAB surface density on PSS solution. The symbols indicate the concentration and kind of salt in the subphase as well as the PSS chain length (circle, 0.01 M; inverse triangle, 0.1 M; square, long PSS on 1 M; diamond, short PSS on 1 M; solid symbols correspond to NaCl and open to CsCl). The straight line at high surface densities corresponds to 860 Å³, the volume of two ordered C_{17} alkyl chains. These measurements were taken in the compressed phase, beyond the plateau region. The straight line at low surface densities is a fit to the data obtained in the expanded phase and yields a tail volume of 1000 Å³, a value which agrees well with disordered alkyl chains.

The constraint concerning the tail electrons is maintained. To further reduce free parameters, we assume that the PSS1 and PSS2 slabs exhibit the same thickness, yet different electron densities. Together with one common roughness for all interfaces, there are five free parameters. (Similar electron density profiles with two instead of three slabs can be obtained with more roughnesses, yet the parameters are more interdependent on each other—therefore, this approach was abandoned.)

A representative series of electron density profiles together with the slab assignment is depicted in Figure 8. As expected, on compression, the lipid tail thickness increases. The lengths of the PSS1 and PSS2 slabs remain essentially constant (because of model constraints, they are identical, too), 10.8 ± 0.2 Å (averaged over 51 measurements), a value which compares well with the 12 Å, known as the diameter of a PSS chain.[35,36]

This finding suggests a high-density 2-dimensional polymer coil beneath the DODAB monolayer, and there are indications of a second, low-density polymer monolayer beneath the first one. Obviously, the ammonium headgroup of the DODAB is located slightly above and between the first polymer monolayer.

The electron density contrast of both PSS slabs appears to be due to cation incorporation; it is much larger on CsCl than on NaCl solution. Actually, the counterion dependence is more unambiguous for the PSS2 slab whose electron density increases on compression. In contrast, the electron density of the PSS1 slab shows a pronounced decrease on compression, an effect which has to be attributed to cation removal. The PSS is neutralized by DODAB molecules and by cations; the exact ratio depends on the DODAB molecular area and, on compression, is shifted in favor of the DODAB. Obviously, the replacement of the counterions by DODAB is limited to the PSS1 slab.

The thick and diffuse polymer layer described by a Gaussian (≈70 Å) exceeds the scale of Figure 8; it causes the depicted (apparent) increase of the subphase electron density. The analysis reveals that the diffuse polymer layer thins on compression and eventually disappears, at a molecular area of about 80 Å².

Before discussing the polyelectrolyte density profile, it is important to verify that the DODAB parameter assignment is reasonable. Therefore, in Figure 9 the thickness of the hydrophobic tail is shown as a function of the DODAB surface coverage (i.e., inverse molecular area). Because of the constraint (constant amount of electrons), there is almost no scatter. The straight line at high surface densities corresponds to the theoretical molecular volume of two condensed C_{17} alkyl chains, $(1.5 + 16 \times 1.25) \times 40$ Å³ = 860 Å³ (beyond the plateau region). The straight line at low surface densities is calculated from a linear fit to the data measured in the expanded phase and corresponds to a volume of 1000 Å³. These changes in the alkyl chain volume correspond to a tail ordering transition which occurs even after PSS adsorption. Compared to DODAB without PSS, the tail slab is 3−5 Å thicker. Together with the fact that the introduction of a constant amount of electrons in the tail slab is now feasible (which was impossible without the PSS), we conclude that the whole alkyl chain now belongs to the tail slab—without the PSS, the headgroup slab was increased on the expense of the tail slab. This effect was caused by the Cl^- anions situated between and above the ammonium groups. In contrast, the PSS is situated mostly beneath the ammonium groups.

The aim of the experiments is to obtain a detailed segment density profile of the adsorbed PSS. Thus, one would like to know in each PSS slab how many PSS monomers and water molecules correspond to one surface charge (i.e., DODAB molecule). Known parameters are the PSS monomer volume (210 Å³), the counterions Cs^+ (38 Å³) and Na^+ (0.5 Å³, this value is so low because Na^+ is strongly hydrated[37]), the water (30 Å³), the molecular volume of the DODAB headgroup (740 Å³) as derived from the isolated monolayer, and the tail volume as calculated above. For each PSS slab the amount of electrons and the volume are known variables. Furthermore, we assume charge compensa-

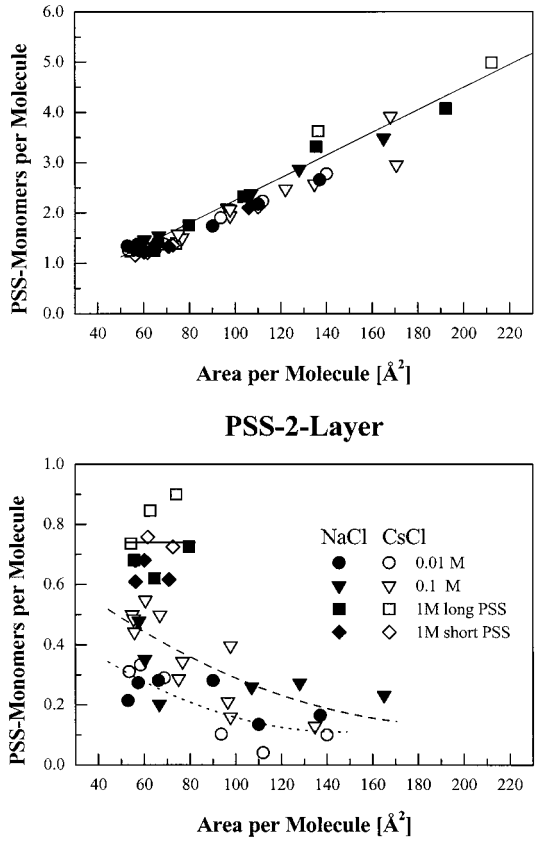

Figure 10. PSS monomers per DODAB molecule as a function of area per surface charge in the (top) PSS1 and (bottom) PSS2 slabs calculated according to eqs 3 and 4, respectively. The straight line in the top figure corresponds to a surface coverage of 0.225 PSS monomers/Å^2 (44 Å^2/monomer). In the bottom figure, the lines are guides to the eye to estimate the surface coverage at the different ionic strengths (dotted line, 0.01 M; dashed line, 0.1 M; straight line, 1 M).

tion and obtain for the PSSi slab the number of electrons E_i and volume V_i

$$E_1 = \rho_1 V_1 = E_{\text{DODAB-head}} + n_{\text{PSS1}} E_{\text{PSS}} + (n_{\text{PSS1}} - 1)E_{\text{cation}} + n_{\text{H}_2\text{O}_1} E_{\text{H}_2\text{O}}$$

$$V_1 = V_{\text{DODAB-head}} + n_{\text{PSS1}} V_{\text{PSS}} + (n_{\text{PSS1}} - 1)V_{\text{cation}} + n_{\text{H}_2\text{O}_1} V_{\text{H}_2\text{O}} \quad (3)$$

and for the PSS2 slab

$$E_2 = \rho_2 V_2 = n_{\text{PSS2}}(E_{\text{PSS}} + E_{\text{cation}}) + n_{\text{H}_2\text{O}_2} E_{\text{H}_2\text{O}}$$

$$V_2 = n_{\text{PSS2}}(V_{\text{PSS}} + V_{\text{cation}}) + n_{\text{H}_2\text{O}_2} V_{\text{H}_2\text{O}} \quad (4)$$

The number of PSS monomers per surface charge (i.e., DODAB molecule) is shown in Figure 10. While the electron density profiles depend strongly on the counterion used, we find the same monomer density profile with the two different cations. Therefore, surface charge neutralization appears to be a valid assumption; furthermore, we can exclude counterion specificity.

In the PSS1 slab directly beneath the monolayer, the monomer coverage appears to be constant and largely independent of the surface charge, 44 Å^2/monomer. Only at surface charge densities exceeding 1 e$^-$/60 Å^2, a slight increase occurs. Note that the PSS1 layer causes a pronounced surface charge overcompensation (1.2−6 PSS monomers per DODAB molecule). On compression, the

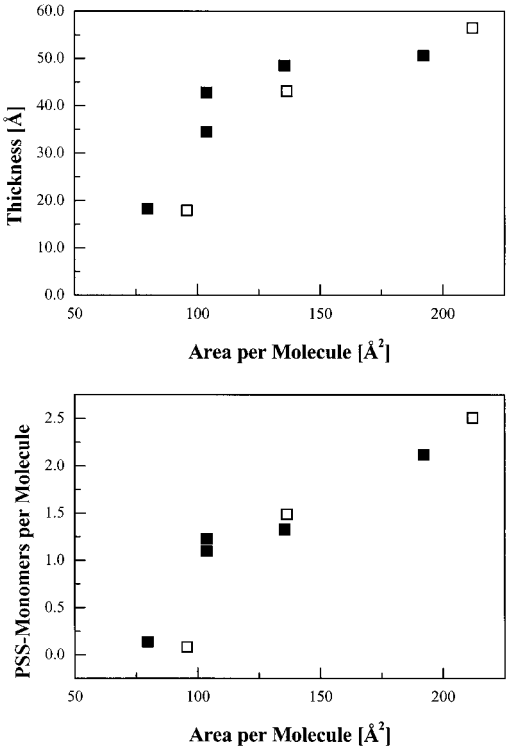

Figure 11. Thick and diffuse PSS layer occurs only at high salt (1 M) and for the high molecular weight PSS (M_w = 77 400 Da). Depicted are its (top) thickness as a function of surface charge (i.e., molecular area) and (bottom) the deduced surface coverage. Symbol assignment as in Figure 10.

constant negative chain charge of the PSS monolayer is progressively neutralized by low-contrast DODAB instead of by electron-rich monovalent counterions. Therefore, the electron density of this slab and thus the height of the first maximum in the reflectivity curves decrease.

In the PSS2 slab, which we tentatively describe as a second monolayer further down into the water, the monomer density is much smaller than in the PSS1 slab. Again, no ion specificity is found. However, the surface coverage depends strongly on the salt concentration: On increase of the surface charge density it amounts to 0.1−0.3 PSS monomers per DODAB molecule for 0.01 M salt, 0.2−0.5 for 0.1 M, and 0.8−1 for 1 M (in the compressed phase). (Note that at high salt the X-ray contrast decreases because of the increased subphase electron density.) For the high salt concentration and low molecular area, it is impossible to distinguish between the PSS2 layer and the diffuse extended layer.

The characteristic parameters of the thick and diffuse surface layer are depicted in Figure 11. This layer is only in evidence at 1 M salt and for the high molecular weight PSS. The good agreement found for the different types of salts is rather amazing given the weakness of the first minimum in the reflectivity curves. (Our method of counterion labeling is only sensitive to about 1 vol %.) The thickness of the diffuse layer decreases with increasing surface charge density (i.e., area per DODAB molecule) and disappears at ca. 80 Å^2. The maximum coil thickness observed is about 60 Å. The PSS coverage from the coils is almost constant at areas exceeding ca. 100 Å^2. No diffuse polymer layer was found for the low molecular weight polymer with a contour length of 52 Å, suggesting that the polymer surface persistence length l_{eff} is larger than 52 Å.

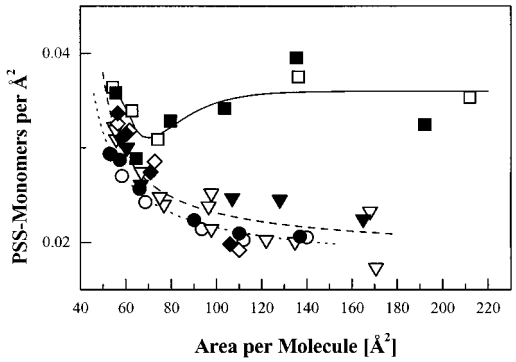

Figure 12. Total PSS coverage as a function of surface charge (i.e., DODAB molecular area). Symbol assignment as in Figure 10. The lines are guides to the eye to estimate the surface coverage at the different ionic strengths (dotted line, 0.01 M; dashed line, 0.1 M; straight line, 1 M).

Summary of the Observed Polymer Structure. The electron density profile of the adsorbed polymer depends on both surface charge and salt concentration: There is no resolvable ion specificity for monovalent ions. The PSS adsorbs basically as 2-dimensional coils with many chain crossings. In the electron density profile, this looks like a first "full" monolayer (with constant surface coverage), yet both the first and second monolayer are necessary to neutralize the surface charge. The thickness of each PSS monolayer slab corresponds to one PSS chain diameter. The PSS density within the second monolayer is generally smaller than within the first one and increases with both the surface charge density and the salt concentration. Additionally, at 1 M salt an extended diffuse polymer layer with a maximum thickness of 60 Å is observed, provided the polymer is long enough. The diffuse layer shrinks with increasing surface charge density until it disappears at 80 Å^2 DODAB molecular area.

Therefore, the total surface coverage of PSS monomers per unit area (cf. Figure 12) shows a rich and even nonmonotonic behavior. At low salt it increases with the surface charge density. The salt increase from 0.01 to 0.1 M causes a slight increase in PSS coverage mainly at high surface charge density ($>e^-$/70 Å^2). At low surface charge and high salt (1 M), a strong overall increase is found for the long polymer due to the formation of a diffuse extended adsorption layer. On compression the PSS coverage is first constant, and then coiled polymers desorb until the surface charge is increased to e^-/80 Å^2. On further compression, polymers adsorb again, but only in a flat conformation. The highest PSS coverage is found for DODAB molecular areas exceeding 120 Å^2, in the constant coverage regime.

Finally, note that the time scale necessary to achieve the equilibrium conformation of the polymers is below 2 h, whereas on solids substrates it is 4 days.[3] This is due to the additional degree of freedom supplied by the lateral mobility of liquid surfaces.

Discussion

Pure Monolayer. First, we would like to discuss briefly the structure profile of the pure DODAB monolayers. It is very unexpected to find the counterions of a charged amphiphile between the alkyl chains and effectively shortening the hydrophobic moiety. For all other lipids and fatty acids studied so far, the counterions were found beneath the headgroups.[31] Also, these structural findings disagree with the standard assumption of DLVO theory: a charged interface neutralized by a diffuse layer of counterions. Instead, the dependence of the hydrophobic/hydrophilic interface within the monolayer can explain the well-known ion specifity of DODAB monolayers:[24] If the OH^- or F^- concentration in the subphase is high, DODAB remains in the fluid phase. With Cl^- or Br^-, a temperature-dependent chain ordering transition is observed, similar to those in Figure 2. With J^- (iodine), the DODAB tails remain frozen. Thus, decreasing anion size liquefies the monolayer, because the anions penetrate the hydrophobic part of the monolayer and effectively prevent alkyl chain ordering. This effect appears to be specific to DODAB with its small headgroup area, compared to the hydrophobic alkyl tails. The PSS chains are large anions, which cannot penetrate into the monolayer. Now, the hydrophobic molecular parts can be identified in the electron density profile (cf. Figure 9).

Table 1. Comparison between PSS Surface Coverage on Different Solid Surfaces[43,44] As Described in the Literature and Our Work at Different Surface Charges

	Schmitt (1996)[43] [mg/m^2]	Cosgrove (1986)[44] [mg/m^2]	this work (low surf. charge)	this work (e^-/50 Å^2)
no salt (0.01 M)	0.55	0.2−0.88	0.68	0.85−0.91
1 M	1.16	1.36−2.2	1.21−1.51	1.07

In principle, one has to distinguish between chemically bound counterions and those which are mobile and screen the chain charge on length scales of the Debye length $1/\kappa$. However, with X-ray reflectivity, we cannot distinguish between chemically bound and electrostatically attracted, mobile counterions. While we would like to think of the DODAB monolayer as a homogeneously charged surface, we cannot exclude commensurate binding between PSS monomers and ordered DODAB headgroups.[38] Yet, the electron density profiles obtained with ordered and disordered alkyl tails are very similar. Also, the strong dependence of PSS coverage on ion concentration shows that other effects but short-ranged ion binding are important, too. In contrast to small monovalent anions, the PSS chains show a liquefying effect; the surface pressure increases on addition of polymer and even further on addition of salt. Very likely, this is due to increased monomer binding to the surface; the same effect as found with poly(ethylene glycol) adsorbs onto the surface[39,40] and explained theoretically.[41,42] However, the dependence on polymer length as we find it (cf. Figure 3) is not accounted for.

PSS Coverage on Solid Substrates. To probe the relevance of our results, it is necessary to compare our data obtained with liquid surfaces with the PSS coverage on solid substrates described in the literature. As substrate, glass functionalized with slightly hydrophobic aminobutyl silane[43] (contact angle with water 30°) or polystyrene latices[44] (even though M_w = 780 000 Da) are widely used.[45] The same coverage was found as on liquid DODAB at low surface charge (cf. Table 1). The trends on changing the salt are the same; on solid substrates the PSS coverage doubles on changing from low to high salt (i.e., 1 M) conditions. Also, roughly the same chain conformations are described: flat conformation if adsorbed from low salt, yet coiled from high salt solution.[8,9,46] High surface charge (e^-/50 Å^2) liquid interfaces are very different; the PSS coverage is high already at low salt. Changing to high salt conditions, only a 20% increase is observed, a much smaller effect

than the factor of 2 found at low surface charge or on solid substrates. Furthermore, at high surface charge, the adsorption layer is always flat. In contrast, flat adsorption at high salt was never observed on solid surfaces.

While the similarities between adsorption on solid surfaces and low charge liquid surfaces are striking, one cannot conclude that all solid surfaces exhibit low surface charge. On solid substrates some chain conformations are kinetically trapped. This is evidenced by surface forces apparatus experiments, when coiled chains prepared by adsorption from high salt do not flatten even after hours in low salt.[7,47] Also, irreversible deformation of the diffuse extended layer was reported.[7,47] Since a diffuse extended layer is more similar to the bulk conformation than a flat adsorption layer, the loops and tails observed on solid surfaces may be a transient state which is immobilized.

Comparison to Theories. Theories on polyelectrolyte adsorption predict a slight surface charge overcompensation, leading to a surface potential of the order $kT/e \sim 30$ mV (or a surface charge of $\sim$1000 Å^2).[3,48−50] This deviation from charge neutralization is within the confidence limits of our experiments. Polyelectrolytes at low salt are subject to two attractive forces: electrostatics and image forces, which are predicted to cause flat adsorption.[3,49,50] Image forces are due to the difference between the dielectric constant of water (78) and the substrate (1−2)[49] and repel a charge in water from the interface. Therefore, image forces favor counterion binding. As theoretically predicted, we find largely flat adsorbed PSS neutralized by counterions. Furthermore, theoretically the surface persistence length l_{eff} exceeds the bulk persistence length L_T by a factor of 2.[49,50] For the large molecular weight polymer, the bulk persistence length was found to be $L_T \sim 50$ Å for 1 M salt and $\sim$80 Å for 0.1 M.[4] Thus, a surface persistence length exceeding 52 Å at 1 M salt is very reasonable, as the absence of a diffuse extended layer for the short PSS indicates.

There is a pronounced disagreement with theoretical predictions:[49,50] the surface charge is supposed to be overcompensated by at most a factor of 2. In contrast, we do observe constant PSS coverage in a wide range, and the overcompensation is as large as a factor of 6.

There is also the hydrophobic backbone of PSS to consider: PSS is a slightly hydrophobic polyelectrolyte which adsorbs onto the air/water interface[51] and onto hydrophobic surfaces.[52] Also, it coadsorbs with surfactants at the air/water surface; the composition of the surface layer depends on the bulk PSS concentration.[53] Investigating a diblock copolymer consisting of a hydrophobic and a PSS block, one finds a 2-dimensional PSS layer at the interface between the two blocks, both for diblock copolymer monolayers at the air/water interface[35,54] and for micelles investigated with cryo-TEM.[52] In this case, the PSS monomer density within the monolayer is even larger than in the experiments described above, 35 Å^2/monomer.[35,54] A PSS chain with more bound counterions is less soluble in water, and eventually it precipitates. Therefore, we conclude that hydrophobic forces are the reason for the constant PSS coverage at low surface charge.

If one considers the lateral structure of the adsorbed polyelectrolyte chains at low salt, complex predictions exist:[49] For very large polyelectrolyte surface persistence lengths, the polymers exhibit a 2-dimensional lamellar structure as has been found for DNA.[55] Yet with shortening of the persistence length, the adsorbed layer disorders and chain crossings occur. A multitude of crossings appear in the density profile as a second monolayer. Our findings suggest that we have a "full" first monolayer, and any changes in coverage occur in the PSS2 layer.

We find coverage increase with increasing surface charge density, i.e., increasing electrostatic attraction. That finding is very intuitive. More difficult to understand is the increased coverage with increasing salt (decreasing screening length $1/\kappa$). This can be explained by a decrease in chain charge due to counterion binding. Furthermore, stronger electrostatic screening shortens the surface persistence length and facilitates chain crossings.

Theoretical predictions are only available at low salt conditions, when the electrostatic screening length $1/\kappa$ exceeds the Bjerrum length (7.5 Å); i.e., only long-ranged electrostatic interactions are considered. The electrostatic forces at 1 M CsCl (or NaCl) are very short-ranged, with $1/\kappa = 3$ Å. As found and predicted for uncharged polymers,[3] the thickness of the adsorption layer is smaller than the persistence length and depends sensitively on the strength of attraction of the polymer to the interface, in our case the electrostatics. Yet we do not know whether surface or bulk persistence length is the relevant parameter. Although difficult to understand, high salt experiments are those with highest technological relevance, for instance polyelectrolyte multilayer preparation occurs at these conditions.[56]

Conclusion and Outlook

We found a rich and complex behavior illuminating a few aspects of polyelectrolyte adsorption onto oppositely charged liquid surfaces. PSS adsorbs as a flat layer; with increasing surface charge and ionic strength, coverage increases. This is attributed to the interplay of three different attractive forces: hydrophobic force, image forces, and electrostatic attraction.

Very intriguingly, at high salt (1 M) and low surface charge we find a diffuse extended polymer which thins and eventually disappears on surface charge increase, a clear indication of the importance of electrostatic attraction. Both the thickness of the diffuse layer and its absence for low molecular weight polymer indicate a persistence length above or of the order of 50 Å at 1 M salt. Comparing the PSS coverage on low charge liquid surfaces and on solid substrates, we find a striking similarity at all salt solutions. To find out how general these results are, experiments at even higher salt conditions as well as with different polymers are necessary.

Acknowledgment. We appreciate discussions with and laboratorium space from Manfred Schmidt. Martien Cohen Stuarts ideas are very much appreciated. We thank the DFG (He 1616/7-3,4) and the BMBF (03C0291C/5) for financial support.

References and Notes

(1) Evans, D. F.; Wennerström, H. *The Colloidal Domain: Where Physics, Chemistry, Biology, and Technology Meet*; VCH: Weinheim, 1994.

(2) Hunter, R. J. *Foundations of Colloid Science*; Oxford Science Publications: New York, 1992; Vols. I and II.

(3) Fleer, G. J.; Cohen-Stuart, M. A. C.; Scheutjens, J. M. H. M.; Cosgrove, T.; Vincent, B. *Polymers at Interfaces*; Chapman and Hall: London, 1993.
(4) Förster, S.; Schmidt, M. *Adv. Polym. Sci.* **1995**, *120*, 51−133.
(5) Asnacios, A.; Espert, A.; Colin, A.; Langevin, D. *Phys. Rev. Lett.* **1997**, *78*, 4974−4977.
(6) Claesson, P. M.; Dahlgren, M. A. G.; Eriksson, L. *Colloids Surf. A: Physicochem. Eng. Aspects* **1994**, *93*, 293−303.
(7) Dahlgren, M. A. G.; Claesson, P. M. *Prog. Colloid Polym. Sci.* **1993**, *93*, 206−208.
(8) Dahlgren, M. A. G.; Hollenburg, H. C. M. *Ber. Bunsen-Ges. Phys. Chem.* **1996**, *100*, 1004−1007.
(9) Dahlgren, M. A. G.; Hollenburg, H.; Claesson, P. M. *Langmuir* **1995**, *11*, 4480−4485.
(10) Berndt, P.; Kurihara, K.; Kunitake, T. *Langmuir* **1992**, *8*, 2486−2490.
(11) Lowack, K.; Helm, C. A. *Macromolecules* **1998**, *31*, 823−833.
(12) Ahuja, R. C.; Caruso, P. L.; Möbius, D. *Thin Solid Films* **1994**, *242*, 195−200.
(13) Kunitake, T. *Angew. Chem.* **1992**, *104*, 692−710.
(14) Möhwald, H. *Rep. Prog. Phys.* **1993**, *56*, 653.
(15) Albrecht, O.; Gruler, H.; Sackmann, E. *J. Phys. (Paris)* **1978**, *39*, 301−313.
(16) Vaynberg, K. A.; Wagner, N. J.; Ahrens, H.; Helm, C. A. *Langmuir* **1999**, *15*, 4685−4689.
(17) Israelachvili, J. N. *Intermolecular and Surface Forces*, 2nd ed.; Academic Press: London, 1991.
(18) Baltes, H.; Schwendler, M.; Helm, C. A.; Möhwald, H. *J. Colloid Interface Sci.* **1996**, *178*, 135−143.
(19) Pershan, P. S.; Als-Nielsen, J. *Phys. Rev. Lett.* **1984**, *52*, 759.
(20) Pedersen, J. S. *J. Appl. Crystallogr.* **1992**, *25*, 129−145.
(21) Pedersen, J. S.; Hamley, I. W. *J. Appl. Crystallogr.* **1994**, *27*, 36−49.
(22) Parratt *Phys. Rev.* **1954**, *95*, 359.
(23) Asmussen, A.; Riegler, H. *J. Chem. Phys.* **1996**, *104*, 8159−8164.
(24) Taylor, D. M.; Dong, Y.; Jones, C. C. *Thin Solid Films* **1996**, *285*, 130−133.
(25) Lösche, M.; Helm, C. A.; Mattes, H. D.; Möhwald, H. *Thin Solid Films* **1985**, *133*, 51−64.
(26) Helm, C. A.; Laxhuber, L. A.; Lösche, M.; Möhwald, H. *Colloid Polym. Sci.* **1986**, *264*, 46−55.
(27) Marra, J. *Biophys. J.* **1986**, *50*, 815−825.
(28) Payens, T. *Phillips Res. Rep.* **1955**, *10*, 425.
(29) Bosio, L.; Benattar, J. J.; Rieutord, F. *Rev. Phys. Appl.* **1987**, *22*, 775−778.
(30) Helm, C. A.; Möhwald, H.; Kjaer, K.; Als-Nielsen, J. *Europhys. Lett.* **1987**, *4*, 697−703.
(31) Kjaer, K.; Als-Nielsen, J.; Helm, C. A.; Tippmann-Krayer, P.; Möhwald, H. *J. Phys. Chem.* **1989**, *93*, 3200−3206.
(32) Helm, C. A.; Tippmann-Krayer, P.; Möhwald, H.; Als-Nielsen, J.; Kjaer, K. *Biophys. J.* **1991**, *60*, 1457−1476.
(33) Tronin, A.; Shapovalov, V. *Thin Solid Films* **1998**, *313*, 785−789.
(34) Als-Nielsen, J. *Solid and Liquid Surfaces Studied by Synchrotron X-ray Diffraction*; Blanckenhagen, W. S. A. W., Ed.; Springer: New York, 1986.
(35) Ahrens, H.; Förster, S.; Helm, C. A. *Phys. Rev. Lett.* **1998**, *81*, 4172−4175.
(36) Donath, E.; Walter, D.; Shilov, V. N.; Knippel, E.; Budde, A.; Lowack, K.; Helm, C. A.; Möhwald, H. *Langmuir* **1997**, *13*, 5294−5305.
(37) *Handbook of Chemistry and Physics*, 67th ed.; CRC Press: Cleveland, OH, 1986−87.
(38) de Meijere, K.; Brezesinski, G.; Kjaer, K.; Möhwald, H. *Langmuir* **1998**, *14*, 4204−4209.
(39) Baekmark, T. R.; Wiesenthal, T.; Kuhn, P.; Bayerl, T. M.; Nuyken, O.; Merkel, R. *Langmuir* **1997**, *13*, 5521−5523.
(40) Ahrens, H.; Baekmark, T. R.; Merkel, R.; Schmitt, J.; Graf, K.; Raiteri, R.; Helm, C. A. *ChemPhysChem* **2000**, *1*, 101−106.
(41) Currie, E. P. K.; Leermakers, F. A. M.; Stuart, M. A. C.; Fleer, G. J. *Macromolecules* **1999**, *32*, 487−498.
(42) Faure, M. C.; Basserau, P.; Carignano, M. A.; Szleifer, I.; Gallot, Y.; Andelman, D. *Eur. Phys. J. B* **1998**, *3*, 365−375.
(43) Schmitt, J. Aufbau und strukturelle Charakterisierung von Multilagen aus Polyelektrolyten, Reaktivpolymeren und Kolloiden. Thesis, Johannes Gutenberg-Universität, Mainz, 1996.
(44) Cosgrove, T.; Obey, T. M.; Vincent, B. *J. Colloid Interface Sci.* **1986**, *111*, 409−418.
(45) Schlenoff, J. B.; Li, M. *Ber. Bunsen-Ges. Phys. Chem.* **1996**, *100*, 943−947.
(46) von Klitzing, R.; Möhwald, H. *Langmuir* **1995**, *11*, 3554−3559.
(47) Dahlgren, M. A. G.; Waltermo, Å.; Blomberg, E.; Claesson, P. M.; Sjöström, L.; Åkesson, T.; Jönsson, B. *J. Phys. Chem.* **1993**, *97*, 11769−11775.
(48) Stuart, M. A. C. *Polyelectrolytes on Solid Surfaces*; Daillant, J., Guenoun, P., Marques, C., Muller, P., Vân, J. T. T., Eds.; Editions Frontières: Gif-sur-Yvette, France, 1996; pp 1−12.
(49) Netz, R. R.; Joanny, J.-F. *Macromolecules* **1999**, *32*, 9012−9025.
(50) Joanny, J. F. *Eur. Phys. J. B* **1999**, *9*, 117−122.
(51) Yim, H.; Kent, M.; Matheson, A.; Ivkov, R.; Satija, S.; Majewski, J.; Smitth, G. S. *Macromolecules* **2000**, *33*, 6126−6133.
(52) Förster, S.; Hermsdorf, N.; Leube, W., in preparation.
(53) Asnacios, A.; Klitzing, R.; Langevin, D. *Colloids Surf. A* **2000**, *167*, 189−197.
(54) Ahrens, H.; Förster, S.; Helm, C. A. *Macromolecules* **1997**, *30*, 8447−8452.
(55) Maier, B.; Rädler, J. O. *Phys. Rev. Lett.* **1999**, *82*, 1911−1914.
(56) Decher, G. *Science* **1997**, *277*, 1232−1237.
(57) Ruths, J. Organische Mono- und Multischichten an der Wasser/Luft-Grenzfläche: Aufbau, Übertragung, Charakterisierung. Thesis, Johnnes Gutenberg-Universität, Mainz, Germany, 1996.

MA001520H